

High-temperature crustal scale shear zone at the western margin of the Eastern Ghats granulite belt, India: implications for rapid exhumation

S. Bhattacharya

Indian Statistical Institute, 203, B.T.Road., Calcutta 700035, India

Received 16 October 2002; revised 3 October 2003; accepted 3 November 2003

Abstract

A mylonitic shear zone occurs along the western margin of the Eastern Ghats Granulite belt, India. In the northern sector, it separates metapelitic and mafic granulites from the granite gneisses of the Bastar craton, while in the southern sector, it separates charnockitic gneisses and mafic granulites from the granite gneisses of the Bastar craton. This boundary shear zone is characterized by a mylonitic foliation and a stretching lineation. Microstructures characterize high-grade conditions and quartz *c*-axis patterns show strong point maxima close to the long axes of the strain ellipsoids, indicating dominant prism [c] slip in quartz, commonly interpreted in terms of ductile deformation at high-temperatures. Quartz *c*-axis patterns in the recrystallized and unrecrystallized domains also imply grain boundary migration as the principal mechanism of dynamic recrystallization at high temperature conditions. A rapid exhumation during shearing in this marginal part of the convergent Eastern Ghats orogen is indicated by decompression reaction textures and retrograde hydration reactions, presumably due to hydrous fluid ingress, in the shear zone rocks.

Keywords: Granulite belt; Hydration; Quartz

1. Introduction

The boundaries between Precambrian mobile belts and adjacent cratons are important areas in understanding the evolution of such contrasting crustal pairs (Van Reenen et al., 1990; Roering et al., 1992; Perchuk et al., 2000; Smit et al., 2001). The Eastern Ghats Granulite belt (EGGB), bounded by granite–greenstone belts of the Singhbhum and Bastar cratons to the north and west, respectively, provides an excellent opportunity for such a study focussing on the boundary areas. Although structural–petrological studies on granulite facies rocks and some geochronological data have been published during the last decade, those were mostly from different internal segments (Lal et al., 1987; Kamineni and Rao, 1988; Paul et al., 1990; Sengupta et al., 1990; Dasgupta et al., 1992; 1994; Bhattacharya et al., 1994; Sen et al., 1995; Shaw

The western margin of the Eastern Ghats belt was originally described as a boundary fault, on the evidence of a sharp NNE–SSW trending contact against granitic gneisses of the Bastar craton and the presence of crushed rocks in the boundary region (Fermor, 1936). However, Crookshank (1938) described intrusive charnockites with tongues and apophyses into the schist belt of the Bastar craton around Jaypur. Renewed interest and focus on this important problem have been evident during the last decade and are manifested in a number of publications. Nanda (1995) described a transition zone on the evidence of the coexistence of low-grade and high-grade rocks in the boundary region. Nanda (1995) further emphasized that field evidence does not support the view of uplift of the high-grade belt along a boundary fault. Chetty and Murthy (1994) proposed a network of ductile shear zones from Landsat studies, but did not discriminate the boundary shear zones from those occurring within the high-grade belt. Biswal et al. (2000) described a boundary shear zone around Lakhna (location 6 in Fig. 1) and Gupta et al.

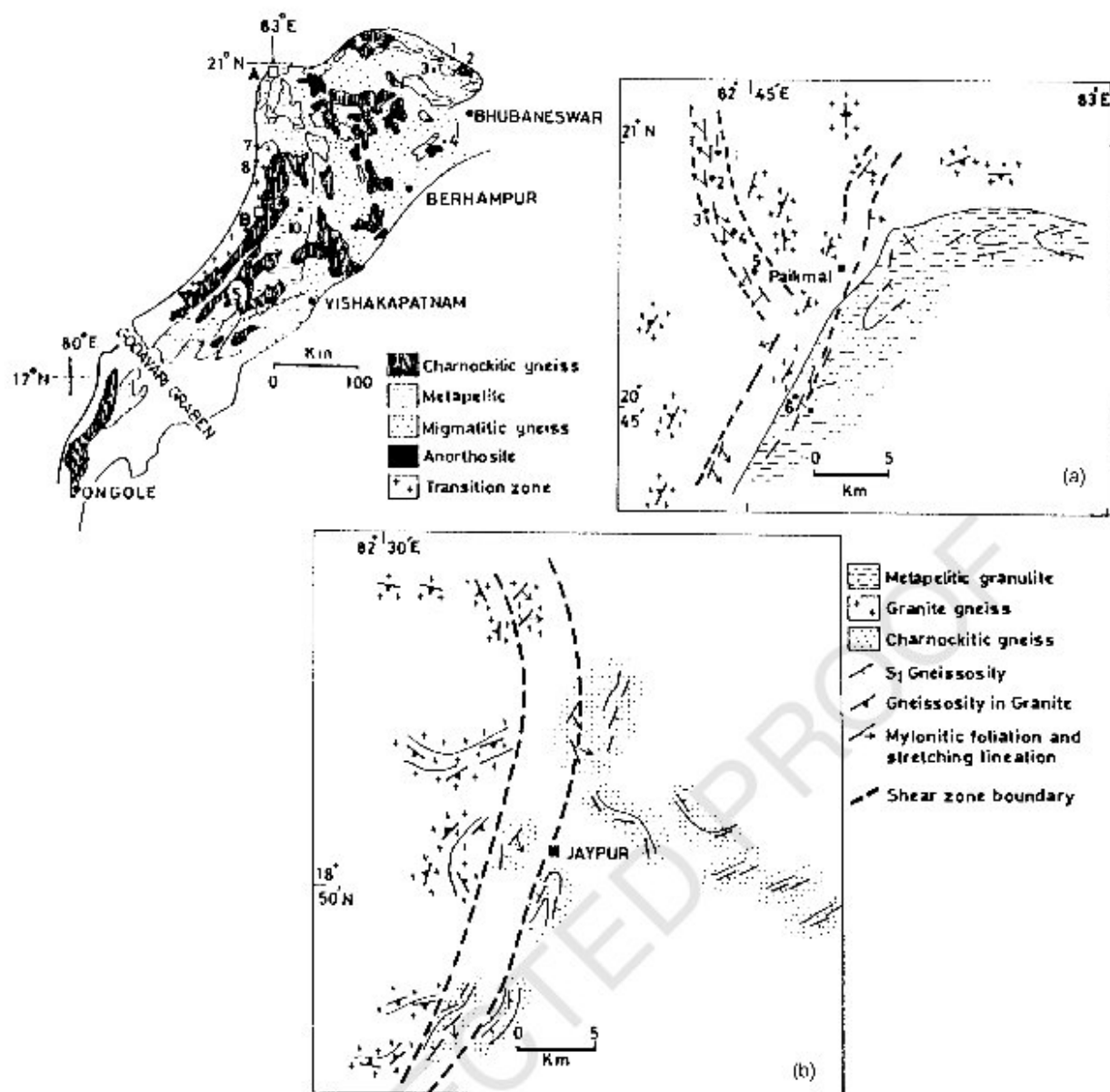


Fig. 1. Generalized geological map of the Eastern Ghats belt, modified after Ramakrishnan et al. (1998). Important locations: 1. Bhuban, 2. Jenapore, 3. Angul, 4. Chilka, 5. Paderu, 6. Paikmal, 7. Deobhog, 8. Lakhna, 9. Jaypur, 10. Korapat. (a) Detailed geological map of the Paikmal area (northern sector): Locations of analyzed samples for quartz *c*-axes, (Fig. 5) 1–6 are also given. (b) Detailed geological map of the Jaypur area (southern sector).

(2000) suggested westward thrusting of the Eastern Ghats over the Bastar craton, based on evidence of (a) an inverted thermal gradient in the cratonic rocks, with complementary cooling and hydration in the granulites, and (b) the sense in which the earlier foliation curves into the shear plane. These authors related the juxtaposition to a late and separate deformation event (D_3), but peak P – T conditions in the granulites were said to have been attained only during this deformation. The cooling and hydration in the granulites during shearing would imply retrogression attendant on the proposed thrusting of the mobile belt over the craton. Although these authors observed mylonites with stretching lineations, they did not use angular

relationships between these mylonitic fabrics (S and C) as shear sense criteria. Kar et al. (2001); Bhattacharya (2002) described mylonitic shear zones at the western margin of the Eastern Ghats belt, from Jaypur in the south and Paikmal in the north, and Bhattacharya (2002) interpreted the shear zone as the result of oblique collision against an irregular continental (passive) margin. Thus a crustal scale shear zone is evident at the western margin of the high-grade Eastern Ghats belt, but a comprehensive understanding of the relation between this shear zone and the evolution of the high-grade belt is still lacking.

This paper presents mesoscopic to microscopic scale structural and petrological evidence across the shear zone,

that could be ascribed to rapid exhumation of the high-grade belt during high-temperature ductile shearing.

2. Geological setting

2.1. Eastern Ghats belt

The lithological make up of the Eastern Ghats belt can be described in terms of three broad groups, namely metapelitic granulites; charnockite–enderbite gneisses and associated granulites; and migmatitic gneisses. Additionally, a transition zone occurs along a significant length of the western margin (Fig. 1, modified after Ramakrishnan et al., 1998). Anorthosites and alkaline complexes are other important rock types in this high-grade belt. Based on the evidence of a NE–SW regional tectonic trend represented by S_1 gneissosity, a steep axial planar foliation, and common structural repetitions, the Eastern Ghats belt could be described as a convergent orogen that evolved under a regional NW–SE directed compression and attendant homogeneous shortening (Bhattacharya et al., 2001).

2.2. Study area

In the northern sector around Paikmal (Fig. 1a, location 6), the high-grade belt is dominantly represented by metapelitic granulites with minor occurrences of mafic granulites and gametiferous granitic gneiss. The cratonic lithologies are granitoids and amphibolites. The mylonitic shear zone is represented by quartzite mylonites, sheared metapelites, mafic granulites and granites.

In the southern sector around Jaypur (Fig. 1b, location 9), the high-grade belt dominantly exposes charnockite–enderbite gneisses and mafic granulites, with minor occurrence of metapelitic granulites and ironstones, particularly at the northeastern corner of the mapped area. The cratonic rock types are granitic gneisses with minor amphibolitic enclaves. The mylonitic shear zone is represented by quartzite mylonites, sheared metapelites, sheared charnockitic gneisses and granitic gneisses.

3. Mesoscopic structures

3.1. Northern sector

The metapelitic gneiss is characterized by a pervasive gneissosity, designated as S_1 , which is axial planar to rootless folds. The S_1 gneissosity displays mesoscopic F_2 folds. Both S_1 and the axial traces of F_2 folds display a bend from E–W in the northeast to NNE–SSW in the southwest (Fig. 1a). In view of the fact that no mesoscopic fold or related axial planar foliation corresponding to this bend could be recognized, the change of

trend is interpreted as a tectonic rotation during collisional juxtaposition of the Eastern Ghats belt against the Bastar craton (Bhattacharya, 2002). The granitoids of the Bastar craton have a crude gneissic foliation, which is at a high angle to the boundary.

The quartzite mylonite has a prominent cleavage type foliation (C-surface of Berthe et al., 1979) and a stretching lineation. The mylonitic banding (S-surface of Berthe et al., 1979) is virtually parallel to the foliation, but asymmetric boudins are occasionally observed on plan view (Fig. 2a). This, and the commonly oblique stretching lineation (Fig. 1a), indicate oblique-slip in the shear zone and are consistent with oblique collisional juxtaposition of the Eastern Ghats belt against the Bastar craton, as suggested by Bhattacharya (2002). Occasionally stretched and dismembered amphibolite layers in small-scale shear zones are observed (Fig. 2b). Two sets of mylonitic foliation, with mean orientations of $342^\circ/70^\circ$ W and $30^\circ/60^\circ$ E, respectively, and with a rake of the stretching lineation typically less than ninety degrees (Fig. 8a and b in Bhattacharya, 2002) and with dextral and sinistral senses of shear on plan view, can be considered as conjugate shear bands C and C', respectively.

3.2. Southern sector

The pervasive gneissic foliation in the charnockitic gneisses is axial planar to rootless folds defined by mafic granulite bands (cf Fig. 2 in Kar et al., 2001) and is designated as S_1 . The S_1 gneissosity commonly displays mesoscopic F_2 folds (Fig. 1b), but axial planar foliation is rarely developed. The mineral foliation in the granite gneisses of the adjoining Bastar craton displays small-scale crenulations and large-scale open folds (Fig. 1b).

The rocks in the boundary region bear the imprint of intense shearing and often develop mylonitic foliation and stretching lineation (Fig. 2c). Also small-scale shear zones are commonly observed in the charnockitic gneisses (Fig. 2d). Folding of mylonitic banding was also observed on the mesoscopic scale, but this did not affect the stretching lineation (cf. Fig. 12 in Kar et al., 2001); prolonged shear displacement on the same shear plane in a highly ductile environment might have developed such folds. The mean orientation of the shear foliation, $340^\circ/70^\circ$ E, and the oblique stretching lineation are consistent with oblique collisional juxtaposition of the Eastern Ghats belt against the Bastar craton in this sector also.

4. Microstructure

4.1. Northern sector

Spectacular microscopic fabrics are observed in the northern sector. In the XZ kinematic section normal to

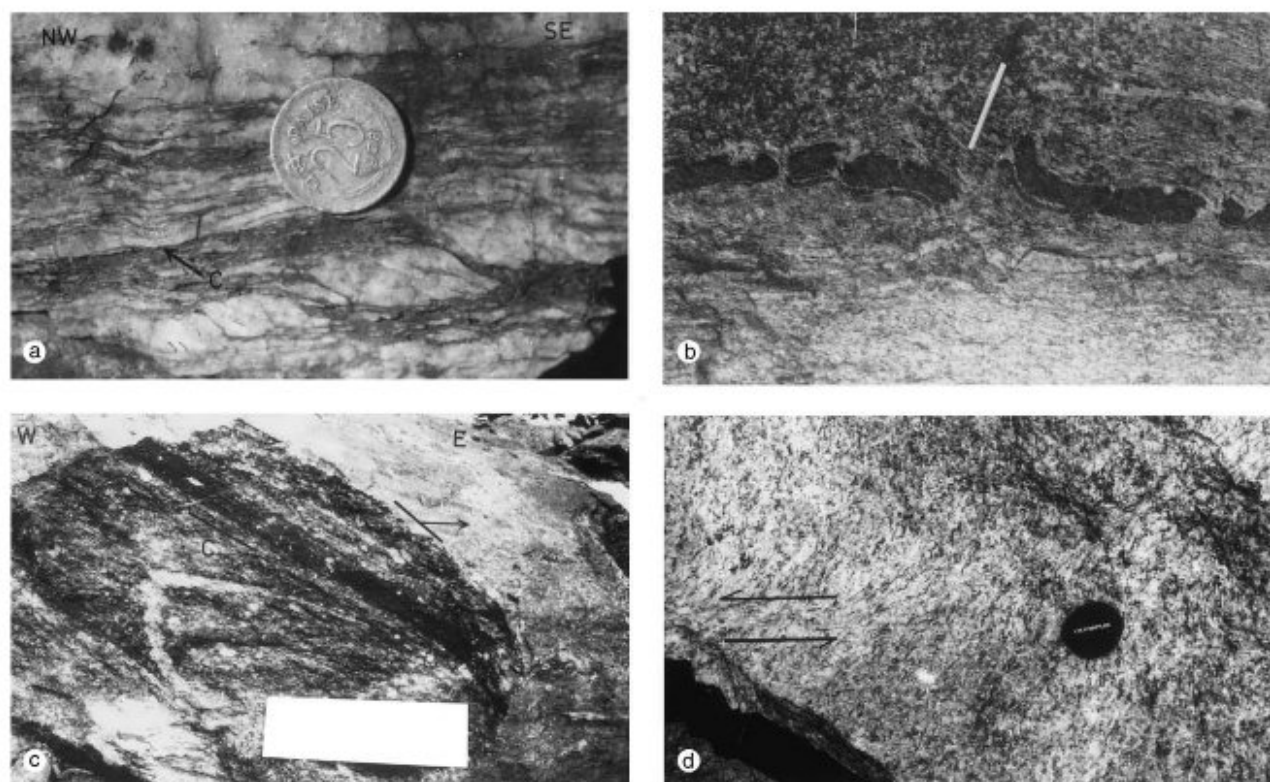


Fig. 2. Field photographs. (a) Asymmetric sigmoidal quartz porphyroblasts in quartzite mylonite, in plan view, showing sinistral micro-duplex stacking. (b) Stretched and dismembered amphibolite layer in a small-scale shear zone developed in granite gneiss, in plan view; the photograph shows a dextral sense of shear with the shear zone striking parallel to the pen at 67°. (c) Mylonitic foliation (cleavage) and oblique stretching lineation in sheared granite gneiss. The sense of shear is dextral. (d) A small-scale shear zone developed in charnockitic gneiss, in plan view. The dextral sense of shear is noted.

foliation and parallel to stretching lineation, the angular relation between S and C indicates a anti-clockwise sense of shear on the westerly plunging lineation (Fig. 3a). Some microstructures in these mylonites could be ascribed to high-grade conditions ($\geq 700^\circ\text{C}$, Blumenfeld et al., 1986). Fig. 3b shows quartz ribbons alternating with recrystallized quartz, where the quartz ribbons represent the shear foliation (C) and the oblique recrystallized quartz represents mylonitic banding (S). Diffuse sub-grain boundaries, presumably due to annealing, also attest to high-grade conditions (Fig. 3c). Lobate and interpenetrating grain boundaries in polycrystalline quartz aggregates in quartzite mylonite (Fig. 3d), and comparable features in the nearby metapelitic granulites with no mylonitic fabric (Fig. 3e) are also indicative of high-temperature conditions during shearing.

4.2. Southern sector

In the sheared granitic gneiss, the pervasive foliation under the microscope is a near continuous cleavage (C-plane) and elliptical quartz–feldspar clasts define the mylonitic banding (S-plane); the angular S–C relation and asymmetric deflection of the external foliation

indicates a clockwise sense of shear (Fig. 4a). In the sheared charnockitic gneisses and mafic granulites, the foliation under the microscope is again continuous cleavage (C-plane) and porphyroclasts of pyroxene and plagioclase represent the mylonitic banding (S-plane). Pyroxene porphyroclasts display a spectacular σ type rolling structure (Passchier and Symptom, 1986) and indicates an anti-clockwise sense of shear (Fig. 4b).

5. Quartz c-axis fabric

In the XZ sections, perpendicular to the shear foliation (C) and parallel to the stretching lineation, quartz c-axis orientations in six samples were measured using a Universal Stage (Fig. 5). Five of these represent domains of dynamic recrystallization (Fig. 5a–e), while one represents old unrecrystallized grains (Fig. 5f). All the samples are characterized by a strong point maximum close to the stretching direction (X). In sample 142 (Fig. 5b), a secondary point maximum close to the compression direction (Z) is also evident. The asymmetric relation between C and S in these sections is also consistent with the clockwise sense of shear.

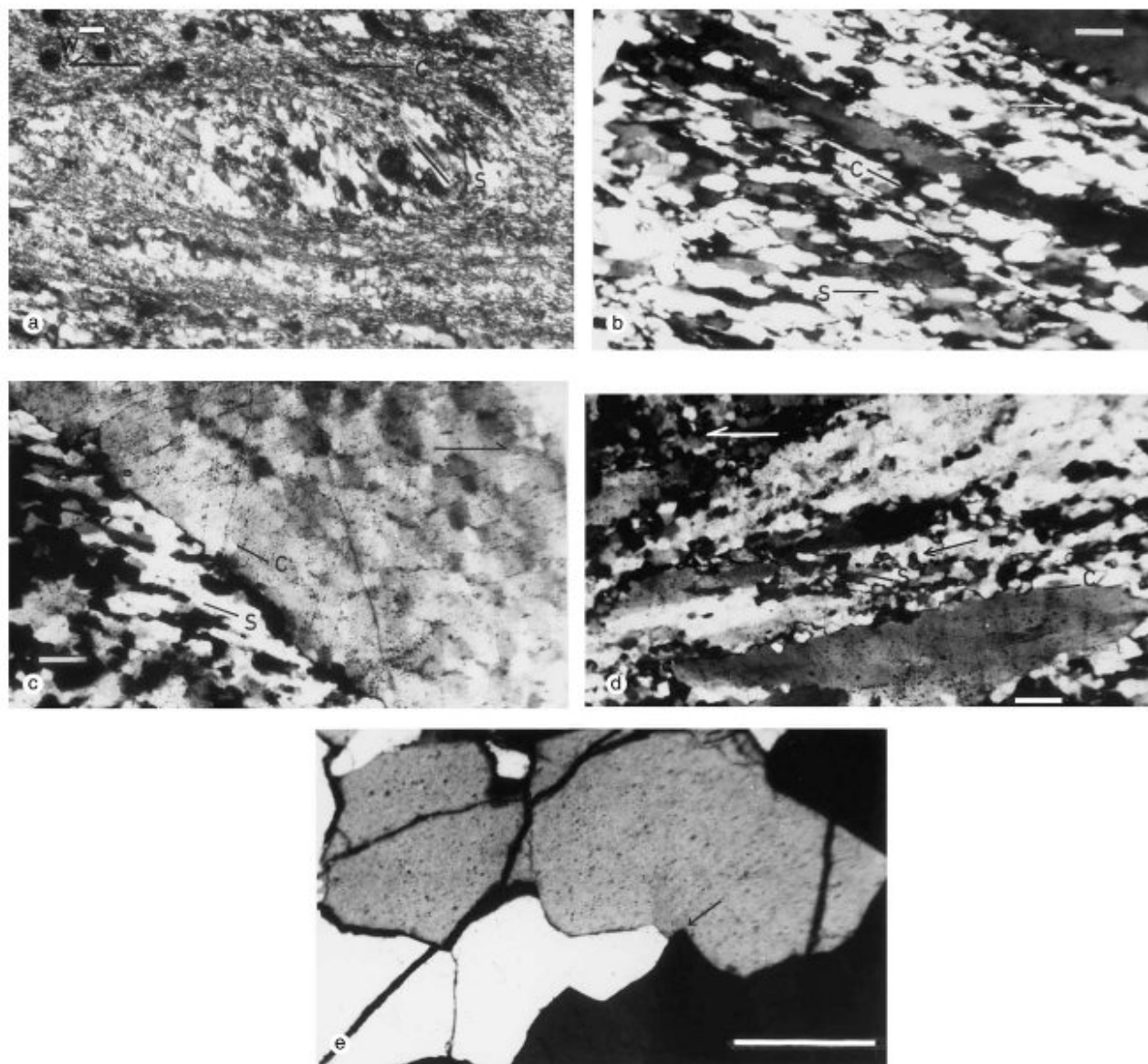


Fig. 3. Photomicrographs. (a) C-type shear bands in a mylonite section normal to foliation and parallel to stretching lineation (XZ kinematic section). S–C relationship indicates an anti-clockwise sense of shear on westerly plunging (arrow) lineation. Scale bar: 7 μ . (b) Quartz ribbons defining shear cleavage or C bands, and recrystallized quartz domains defining mylonitic banding. S. Scale bar: 9 μ . (c) Wide C band with diffuse sub-grain boundaries indicating high temperature annealing. Scale bar: 9 μ . (d) Interpenetrating grain boundaries (arrow) in dynamically recrystallized quartz within quartzite mylonite. Scale bar: 9 μ . (e) Lobate and interpenetrating (arrowhead) grain boundaries in the adjacent metapelitic granulites. Scale bar: 9 μ .

Experimental and observational data suggest that the quartz *c*-axis maxima close to the stretching direction developed due to the dominant activity of prism [c] slip (Blacic, 1975; Linker et al., 1984; Linker et al., 1984; Blumenfeld et al., 1986; Mainprice et al., 1986; Garbutt and Teysier, 1991). The weak point maximum in sample 142 (Fig. 5b) possibly represents associated basal (a) slip. Such a dominant prism [c] fabric is commonly interpreted in terms of high-temperatures (Mainprice et al., 1986; Paterson et al., 1989). It is also significant that the *c*-axis pattern in the recrystallized quartz grains (Fig. 5a–e) does not differ from that in unrecrystallized grains (Fig. 5f). This is characteristic

of high-temperature conditions, when grain boundary migration (GBM) is the dominant recrystallization mechanism (Hirth and Tullis, 1992; Gleason et al., 1993; Rosenberg and Riller, 2000).

In terms of numerical simulation, a single point maximum is analogous to that observed in olivine tectonites (Nicolas and Poirier, 1976). For polycrystalline quartz aggregates, the single point maximum is consistent with the single slip hypothesis (Bouchez et al., 1983), where alignment of the slip direction is toward the *X*-axis of the strain ellipsoid.

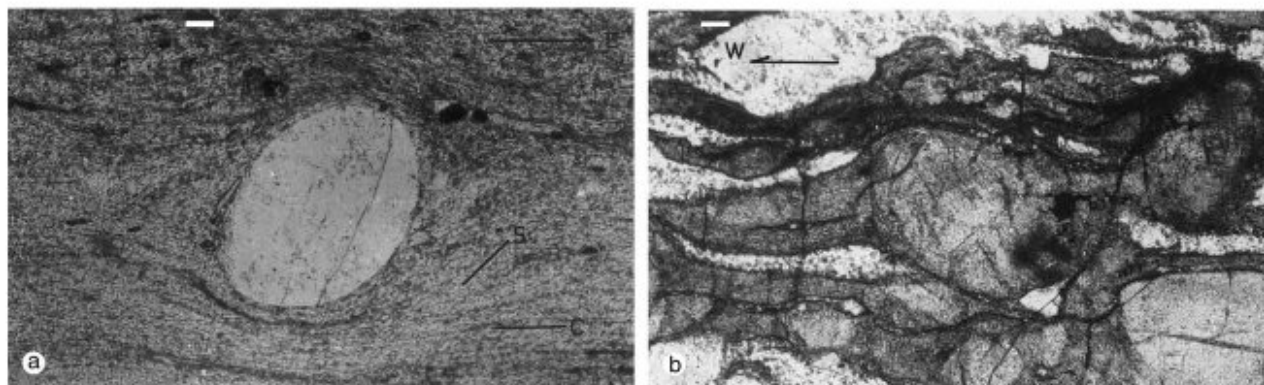


Fig. 4. Photomicrographs. (a) XZ kinematic section in sheared granite gneiss. Feldspar porphyroclasts define the mylonitic banding, S, S–C angular relationship and deflection of external foliation indicating a clockwise sense of shear. Scale bar: 7μ . (b) XZ kinematic section in sheared two-pyroxene granulite, showing typical σ type rolling structure. The sense of shear is anti-clockwise. Scale bar: 7μ .

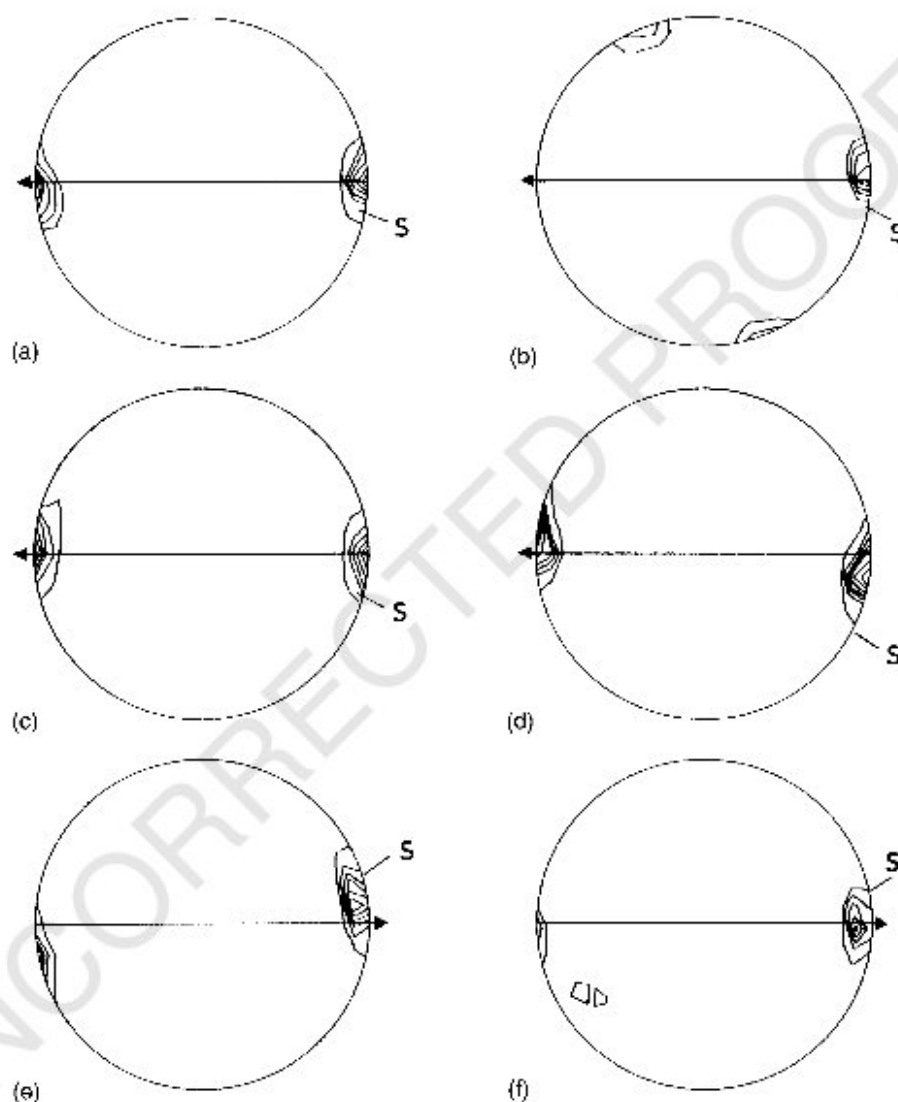


Fig. 5. Lower hemisphere equal area projections for quartz c -axis orientations measured in XZ sections. Fabric patterns are contoured following the Kamb method with $E = \sigma$. Arrow is pointing down plunge of the stretching lineation. Traces of S and C are also marked. (a) Sample 32 (location 5 in Fig. 1a), $N = 180$, contour interval = $6 \times \sigma$, (b) Sample 142 (location 2 in Fig. 1a), $N = 180$, contour interval = $6 \times \sigma$, (c) Sample 150 (location 1 in Fig. 1a), $N = 160$, contour interval = $6 \times \sigma$, (d) Sample 202 (location 4 in Fig. 1a), $N = 200$, contour interval = $6 \times \sigma$, (e) Sample 199 (location 3 in Fig. 1a), $N = 200$, contour interval = $8 \times \sigma$, (f) Sample 177 (location 6 in Fig. 1a), $N = 150$, contour interval = $2 \times \sigma$. Only quartz grains in the unrecrystallized domains were measured in this sample.

6. Petrological constraints

Away from the shear zone, the unshered lithologies such as pelitic and mafic granulites in the northern sector and charnockite and mafic granulite in the southern sector display granoblastic textures, as commonly associated with the early deformation and granulite facies metamorphism in the Eastern Ghats belt (Bhattacharya, 1996, and references therein). Two mafic granulite samples, one each from the two sectors, preserve evidence of garnet–pyroxene–plagioclase–quartz equilibration before exhumation

(Fig. 6a and b). Pressure–temperature estimates of this equilibration were derived using multi-equilibrium calculations (Berman, 1991), using the TWEEQU program. Pressure and temperature for the northern sector (8.2 kbar, 820 °C) and southern sector (9 kbar, 850 °C) were estimated (Table 1). Similar P – T values were reported from several internal segments of the Eastern Ghats belt, as summarized by Sen et al. (1995).

On the other hand, close to the shear zone, these same lithologies display reaction textures that could be ascribed to decompression and tectonic exhumation of the deep

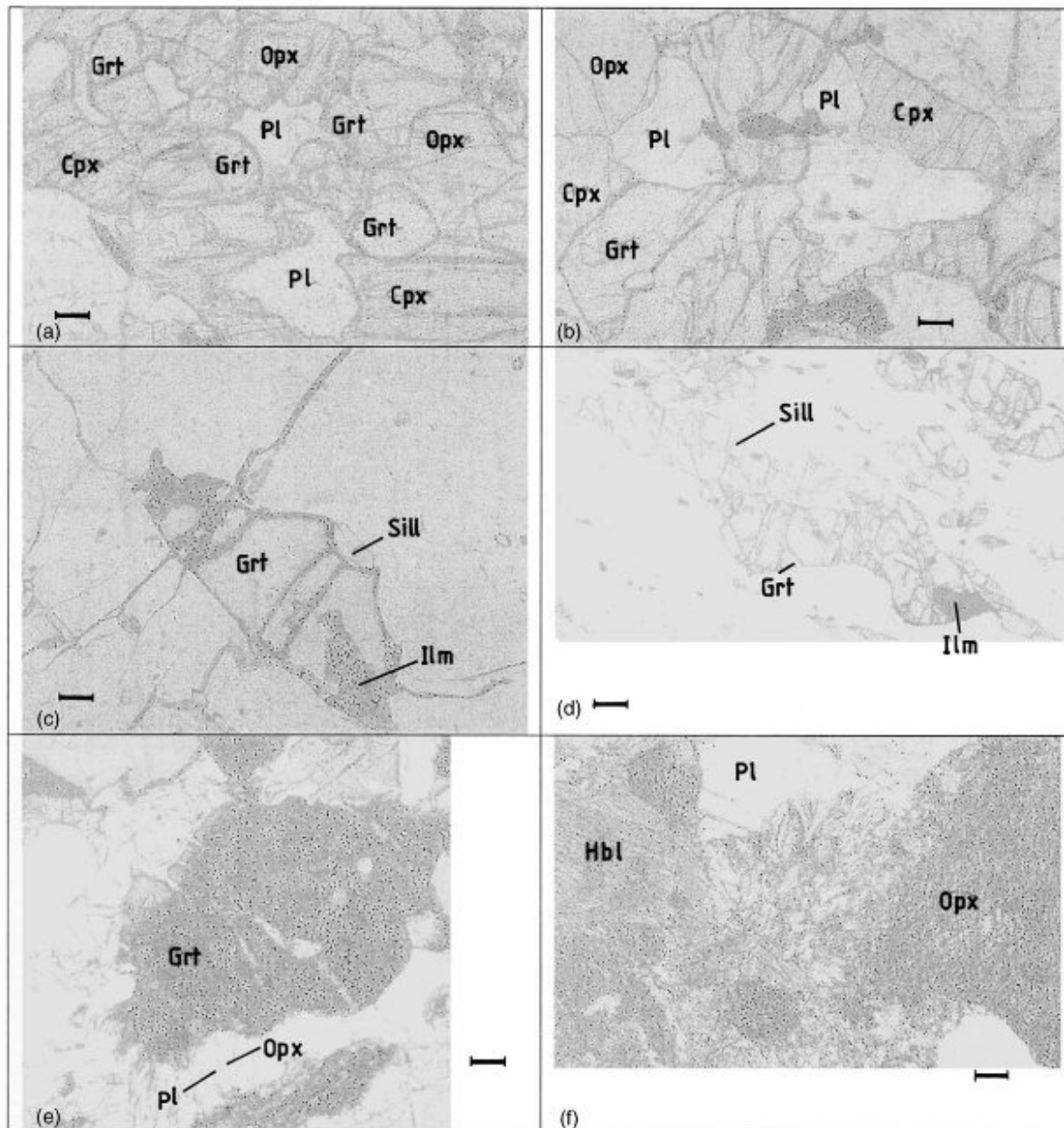


Fig. 6. Photomicrographs. Scale bars 5 μ in each photograph. (a) Granoblastic texture in mafic granulite, showing coexisting garnet–pyroxene–plagioclase + quartz. Note the triple junction indicating equilibrium between these phases. (b) Granoblastic texture in mafic granulite showing coexisting garnet–clinopyroxene–orthopyroxene–plagioclase + quartz. (c) Sillimanite and ilmenite growth on elongate garnet in sheared metapelite. (d) Sillimanite and ilmenite growth on stretched garnet parallel to the stretching lineation, in sheared metapelite. (e) Orthopyroxene–plagioclase symplectitic growth on garnet in a sheared mafic granulite. (f) Biotite–quartz symplectitic growth on an embayed portion of orthopyroxene, in sheared charnockitic gneiss.

Table 1
Coexisting minerals for pressure–temperature estimates

| Sample | P39(Paikmal) | | | J45B (Jaypur) | | | |
|--------------------------------|--------------|----------------|--------|------------------|-------------|--------|---------------|
| | Mineral | Plagioclase | Garnet | Clinopyroxene | Plagioclase | Garnet | Clinopyroxene |
| <i>Oxides</i> | | | | | | | |
| SiO ² | 58.79 | 37.43 | 50.75 | 44.37 | 34.76 | 51.8 | |
| Al ₂ O ₃ | 25.17 | 22.26 | 2.58 | 34.74 | 21.9 | 1.97 | |
| FeO | 0 | 27.01 | 10.07 | 0.04 | 26.85 | 8.61 | |
| MnO | 0 | 0.81 | 0.07 | 0.02 | 0.68 | 0.15 | |
| MgO | 0 | 5.65 | 12.05 | 0.05 | 6.31 | 13.58 | |
| CaO | 7.67 | 6.6 | 21.42 | 18.79 | 8.32 | 23.06 | |
| Na ₂ O | 6.55 | 0 | 0.6 | 1.26 | 0.12 | 0.1 | |
| K ₂ O | 0.23 | 0 | 0 | 0.05 | 0.01 | 0 | |
| TiO ₂ | 0 | 0 | 0.39 | 0.28 | 0.11 | 0.11 | |
| Total | 98.41 | 99.76 | 97.94 | 99.59 | 99.04 | 99.37 | |
| <i>P–T</i> estimates | | 9 kbar, 850 °C | | 8.2 kbar, 820 °C | | | |

crustal granulites during shearing. Pelitic granulites in both sectors display growth of sillimanite and ilmenite at the border of elongate garnet parallel to the stretching lineation (Figs. 6c and d). In view of the gentle positive slope of the reaction garnet + rutile → ilmenite + sillimanite + quartz, a decompression can be inferred from this texture. Mafic granulites in the northern sector show a characteristic orthopyroxene-plagioclase symplectite on an embayed portion of garnet, indicating a reaction such as garnet + quartz → orthopyroxene + plagioclase, and a decompression can be inferred from this texture (Fig. 6e). Sheared charnockitic gneisses in the southern sector commonly display retrogression and hydration; biotite-quartz symplectitic growth on orthopyroxene could indicate hydrous fluid ingress during shearing (Fig. 6f).

7. Discussion

Although reaction textures indicative of decompression have been described from several internal segments of the Eastern Ghats belt (Lal et al., 1987; Dasgupta et al., 1994; Sen et al., 1995; Bhattacharya and Kar, 2002), the kinematics of exhumation in these segments are not well understood. On the other hand, although small-scale shear zones and shear fabrics are commonly observed in several areas (Bhattacharya et al., 1994; Bhattacharya, 1997), the significance of these fabrics in terms of the evolution of the granulite belt is not unequivocally established. Chetty and Murthy (1994) proposed an early collisional regime and suggested that granulite metamorphism was achieved by thrusting. However, based on evidence of subvertical early foliation and reclined folds, Bhattacharya (1996) argued for homogeneous shortening rather than thrusting as the cause of granulite facies metamorphism in the Eastern Ghats belt.

In terms of exhumation of deep crustal rocks in a convergent orogen, Thompson et al. (1997) proposed

from modeling constraints that weak marginal zones will be separated by extensional faults or shear zones, from the much more slowly uplifted rocks of the core of the thickened mountain belt. Although isotopic data on the exhumation history of the Eastern Ghats belt, is sparse, the data from one internal segment have significant implications. Bhattacharya et al. (2003) described a prolonged decompression and reaction history from a single sample, coupled with isotopic disequilibrium between whole rock and minerals in the same sample. This and the time gap of about 100 million years between the end of thickening-related heating (10 kbar, 1000 °C) and the beginning of isobaric cooling (8 kbar, 950 °C), could thus imply a slow exhumation in this internal segment of the Eastern Ghats belt. The crustal scale shear zone at the western margin of the Eastern Ghats belt, with evidence of decompression reactions, could have resulted in much faster exhumation by tectonic denudation, as suggested in the model of Thompson et al. (1997).

8. Conclusions

High-temperature shear zone at the western margin of the Precambrian Mobile belt of the Eastern Ghats, India, could have developed during exhumation of deep crustal granulites. Future isotopic data from this shear zone would provide important constraints on exhumation history in this marginal segment of the regional granulite belt of the Eastern Ghats.

9. Uncited reference

Records of the Geological Survey of India.

Acknowledgements

This study was undertaken in connection with a research project, funded by the Department of Science and Technology, Govt. of India. The Indian Statistical Institute, Calcutta, provided infra structural facilities. Critical comments and suggestions of C.A. Smit and another anonymous reviewer, are thankfully acknowledged.

References

Berthe, D., Choukroune, P., Jegouzol, P., 1979. Orthogneiss, mylonite and non-coaxial deformation of granite: the example of the South Ammonian shear zone. *Journal of Structural Geology* 1, 31–42.

Berman, R.G., 1991. Thermobarometry using multi-equilibrium calculations: a new technique, with petrological applications. *Canadian Mineralogist* 29, 833–855.

Bhattacharya, S., 1996. Eastern Ghats granulite terrain of India: an overview. *Journal of Southeast Asian Earth Sciences* 14, 165–174.

Bhattacharya, S., 1997. Evolution of the Eastern Ghats granulite belt of India in a compressional tectonic regime and juxtaposition against iron ore craton of Singhbhum by oblique collision–transpression. *Proceedings of the Indian Academy of Sciences Earth and Planetary Science* 106, 65–75.

Bhattacharya, S., 2002. Nature of trijunction in the east Indian Precambrians: example from the Eastern Ghats Granulite belt, Singhbhum craton and Bastar craton around Paikmal, western Orissa. *Gondwana Research* 5, 53–62.

Bhattacharya, S., Sen, S.K., Acharyya, A., 1994. The structural setting of the Chilka Lake granulite–migmatite–anorthosite suite with emphasis on the time relation of charnockites. *Precambrian Research* 66, 393–409.

Bhattacharya, S., Kar, R., Misra, S., Teixeira, W., 2001. Early Archaean continental crust in the Eastern Ghats granulite belt, India: isotopic evidence from a charnockite suite. *Geological Magazine* 138, 609–618.

Bhattacharya, S., Kar, R., 2002. High-temperature dehydration melting and decompressive P – T path in a granulite complex from the Eastern Ghats, India. *Contributions to Mineralogy and Petrology* 143, 175–191.

Bhattacharya, S., Kar, R., Teixeira, W., Basei, M., 2003. High-temperature crustal anatexis in a clockwise P – T – t path: isotopic evidence from a granulite–granitoid suite in the Eastern Ghats belt, India. *Journal of the Geological Society, London* 160, 39–46.

Biswal, T.K., Jena, S.K., Datta, S., Das, R., Khan, K., 2000. Deformation of terrane boundary shear zone (Lakhna shear zone) between Eastern Ghats Mobile Belt and Bastar craton in Balangir and Kalahandi districts, Orissa. *Journal of the Geological Society, India* 55, 367–380.

Blaicic, J.D., 1975. Plastic deformation mechanisms in quartz: the effect of water. *Tectonophysics* 27, 271–294.

Blumenfeld, P., Mainprice, D., Bouchez, J.L., 1986. C-slip in quartz from subsolidus deformed granite. *Tectonophysics* 127, 97–115.

Bouchez, J.L., Lister, G.S., Nicolas, A., 1983. Fabric asymmetry and shear sense in movement zones. *Geologisch Rundschau* 72, 401–419.

Chetty, T.R.K., Murthy, D.S.N., 1994. Collision tectonics in the late Precambrian Eastern Ghats Mobile belt: Mesoscopic to satellite scale structural observations. *Terra Nova* 6, 72–81.

Crookshank, H., 1938. The western margin of the Eastern Ghats in southern Jaypur. *Records of the Geological Survey of India*, 73, 398–434.

Dasgupta, S., Sengupta, P., Fukuoka, M., Chakrabarti, S., 1992. Dehydration melting, fluid buffering and decompressional P – T path

in a granulite complex from the Eastern Ghats, India. *Journal of Metamorphic Geology* 10, 777–788.

Dasgupta, S., Sanyal, S., Sengupta, P., Fukuoka, M., 1994. Petrology of granulites from Anakapalle—evidence for Proterozoic decompression in the Eastern Ghats, India. *Journal of Petrology* 35, 433–459.

Fermor, L.L., 1936. An attempt at the correlation of the ancient schistose formations of Peninsular India. *Memoir of the Geological Survey of India* 70.

Garbutt, J.M., Teysier, C., 1991. Prism slip in quartzites of the Okhurst mylonite belt, California. *Journal of Structural Geology* 13, 657–666.

Gleason, G.C., Tullis, J., Heidelbach, H.F., 1993. The role of dynamic recrystallisation in the development of lattice preferred orientation in experimentally deformed quartz aggregates. *Journal of Structural Geology* 15, 1145–1168.

Gupta, S., Bhattacharya, A., Raith, M., Nanda, J.K., 2000. Contrasting pressure-temperature-deformation history across a vestigial craton-mobile belt boundary: the Western margin of the Eastern Ghats belt at Deobhog, India. *Journal of Metamorphic Geology* 18, 683–697.

Hirth, G., Tullis, J., 1992. Dislocation creep regimes in quartz aggregates. *Journal of Structural Geology* 14, 145–159.

Kamineni, D.C., Rao, A.T., 1988. Sapphirine granulites from Kakanuru area, Eastern Ghats, India. *American Mineralogist* 73, 692–700.

Kar, R., Swain, A., Bhattacharya, S., 2001. Nature of craton-mobile belt boundary: an example from Bastar craton-Eastern Ghats Mobile belt contact around Jaypur, Orissa, India. *Indian Journal of Geology* 73, 107–118.

Lal, R.K., Ackermann, D., Upadhyay, H., 1987. P-T-X relationships deduced from corona textures in sapphirine–spinel–quartz assemblages from Paderu, Southern India. *Journal of Geology* 28, 1139–1168.

Linker, M.F., Kirby, S.H., Ord, A., Christie, J.M., 1984. Effects of compression direction on the plasticity and rheology of hydrolytically weakened synthetic quartz crystals at atmospheric pressure. *Journal of Geophysical Research* 89, 4241–4255.

Mainprice, D., Bouchez, J.L., Blumenfeld, P., Tubia, J.M., 1986. Dominant C-slip in naturally deformed quartz: implications for dramatic plastic softening at high temperature. *Geology* 14, 819–822.

Nanda, J.K., 1995. Boundary relation of Eastern Ghats mobile belt. Abstract, Symposium of the Proterozoic events in East Gondwana, Visakhapatnam, 34–35.

Nicolas, A., Poinier, J.P., 1976. Crystal line plasticity and solid state flow in metamorphic rocks. Wiley, London.

Passchier, C.W., Simpson, C., 1986. Porphyroclasts systems as kinematic indicators. *Journal of Structural Geology* 8, 831–843.

Paterson, S.R., Vernon, R.H., Tobisch, O.T., 1989. A review of criteria for the identification of magmatic and tectonic foliations in granitoids. *Journal of Structural Geology* 11, 349–363.

Paul, D.K., Ray Barman, T., McNaughton, N.J., Fletcher, I.R., Potts, P.J., Ramakrishnan, M., Augustine, P.F., 1990. Archaean-Proterozoic evolution of Indian charnockites: isotopic and geochemical evidence from granulites of the Eastern Ghats belt. *Journal of Geology* 98, 253–263.

Perchuk, L.L., Gerya, T.V., Van Reenen, D.D., Smit, C.A., Krötvov, A.V., 2000. P-T paths and tectonic evolution of shear zones separating high-grade terrains from cratons: examples from Kola Peninsula (Russia) and Limpopo Region (South Africa). *Mineralogy and Petrology* 69, 109–142.

Ramakrishnan, M., Nanda, J.K., Augustine, P.F., 1998. Geological evolution of the Proterozoic Eastern Ghats Mobile belt. *Geological Survey of India, Special Publication no. 44*, 1–21.

Roering, C., Van Reenen, D.D., De Beer, J.H., Smit, C.A., Barton, J.M. Jr., De Wit, M.J., Sletter, E.J., Van Schalkwyk, J.F., Stevens, G., Pretorius, S., 1992. Tectonic model of the evolution of Limpopo belt. *Precambrian Research* 55, 539–552.

Rosenberg, C.L., Riller, U., 2000. Partial-melt topology in statically and dynamically recrystallized granite. *Geology* 28, 7–10.

Sen, S.K., Bhattacharya, S., Acharyya, A., 1995. A multi-stage pressure-temperature record in the Chilka Lake granulites: the epitome of the

| | | |
|------|---|------|
| 1009 | metamorphic evolution of Eastern Ghats, India? <i>Journal of Metamorphic Geology</i> 13, 287–298. | 1065 |
| 1010 | | 1066 |
| 1011 | Sengupta, P., Dasgupta, S., Bhattacharya, P.K., Fukuoka, M., Chakrabarti, S., Bhowmik, S., 1990. Petro-tectonic imprints in the sapphirine granulites from Anantagiri, Eastern Ghats mobile belt, India. <i>Journal of Petrology</i> 31, 971–996. | 1067 |
| 1012 | | 1068 |
| 1013 | | 1069 |
| 1014 | Shaw, R.K., Arima, M., Kagami, H., Fanning, C.M., Shiraishi, K., Motoyoshi, Y., 1997. Proterozoic events in the Eastern Ghats belt, India: evidence from Rb–Sr, Sm–Nd systematics and SHRIMP dating. <i>Journal of Geology</i> 105, 645–656. | 1070 |
| 1015 | | 1071 |
| 1016 | | 1072 |
| 1017 | | 1073 |
| 1018 | | 1074 |
| 1019 | | 1075 |
| 1020 | | 1076 |
| 1021 | | 1077 |
| 1022 | | 1078 |
| 1023 | | 1079 |
| 1024 | | 1080 |
| 1025 | | 1081 |
| 1026 | | 1082 |
| 1027 | | 1083 |
| 1028 | | 1084 |
| 1029 | | 1085 |
| 1030 | | 1086 |
| 1031 | | 1087 |
| 1032 | | 1088 |
| 1033 | | 1089 |
| 1034 | | 1090 |
| 1035 | | 1091 |
| 1036 | | 1092 |
| 1037 | | 1093 |
| 1038 | | 1094 |
| 1039 | | 1095 |
| 1040 | | 1096 |
| 1041 | | 1097 |
| 1042 | | 1098 |
| 1043 | | 1099 |
| 1044 | | 1100 |
| 1045 | | 1101 |
| 1046 | | 1102 |
| 1047 | | 1103 |
| 1048 | | 1104 |
| 1049 | | 1105 |
| 1050 | | 1106 |
| 1051 | | 1107 |
| 1052 | | 1108 |
| 1053 | | 1109 |
| 1054 | | 1110 |
| 1055 | | 1111 |
| 1056 | | 1112 |
| 1057 | | 1113 |
| 1058 | | 1114 |
| 1059 | | 1115 |
| 1060 | | 1116 |
| 1061 | | 1117 |
| 1062 | | 1118 |
| 1063 | | 1119 |
| 1064 | | 1120 |
| | Smit, C.A., Van Reenen, D.D., Gerya, T.V., Perchuk, L.L., 2001. P-T conditions of decompression of the Limpopo high-grade terrane: record from shear zones. <i>Journal of Metamorphic Geology</i> 19, 249–268. | |
| | Thompson, A.B., Schulmann, K., Jezek, J., 1997. Extrusion tectonics and elevation of lower crustal metamorphic rocks in convergent orogens. <i>Geology</i> 25, 491–494. | |
| | Van Reenen, D.D., Roering, C., Brundl, G., Smit, C.A., Barton, J.M., 1990. The granulite facies rocks of the Limpopo belt, southern Africa. In: Vielzeuf, D., Vidal, P.H. (Eds.), <i>Granulites and Crustal Evolution</i> , Kluwer, Dordrecht, pp. 257–289. | |